J. Cent. South Univ. (2015) 22: 1191−1202
DOI: 10.1007/s11771-015-2633-4

Springer

Effect laws and mechanisms of different temperatures on isothermal tensile fracture morphologies of high-strength boron steel

LIU Jia-ning(刘佳宁)[1], SONG Yan-li(宋燕利)[2, 3], LU Jue(路珏)[1], GUO Wei(郭巍)[2, 3]

1. School of Materials Science and Engineering, Wuhan University of Technology, Wuhan 430070, China;
2. Hubei Key Laboratory of Advanced Technology of Automotive Parts (Wuhan University of Technology), Wuhan 430070, China;
3. School of Automotive Engineering, Wuhan University of Technology, Wuhan 430070, China

Abstract: The fracture behaviour and morphologies of high-strength boron steel were investigated at different temperatures at a constant strain rate of 0.1 s^{-1} based on isothermal tensile tests. Fracture mechanisms were also analyzed based on the relationship between microstructure transformation and continuous cooling transformation (CCT) curves. It is found that 1) fractures of the investigated steel at high temperatures are dimple fractures; 2) the deformation of high-strength boron steel at high temperatures accelerates diffusion transformations; thus, to obtain full martensite, a higher cooling rate is needed; and 3) the investigated steel has the best plasticity when the deformation temperature is 750 °C.

Key words: high-strength boron steel; fracture morphology; isothermal tensile test

1 Introduction

The hot stamping of high-strength boron steels offers the possibility of greatly reducing vehicle weight and improving safety performance without affecting the performance of the final products, which is very important in attempts to realize lightweight automobiles and thereby reduce energy requirements and emissions [1−3]. Compared with traditional cold forming methods of light-weight materials and their tailor welded blanks [4−8], the hot stamping process effectively overcomes the drawback in formability reduction. However, during the hot stamping process, high-strength boron steels exhibit forming flaws, such as cracks, voids or metallurgical inclusions [9], which seriously restricts the popularisation and application of hot stamping technology. Research on the fracture behaviour and morphologies of high-strength boron steels is crucial for understanding the fracture mechanism.

Many recent studies have focused on the tensile fracture morphologies of steels at room temperature. WANG et al [10] studied the strain rate sensitivity of dual-phase and fully martensitic steel sheets. The experiments showed that all dual-phase steel sheets exhibit positive strain rate sensitivity, while the fully martensitic steel sheets exhibit negative strain rate sensitivity. ARPAN and SOUMITRA [11] quantified the fracture surface morphologies and dimple geometries of tensile fractographs of AISI 304LN stainless steel at various strain rates, finding that at lower strain rates, the dimple density is higher and the dimple diameter is smaller, and vice versa. LU et al [12] found that both the applied strain rate and the LSP impact time strongly affect the ultimate tensile strength, flow stress and fracture morphology of AISI 304 stainless steel. HE [13] reported that the quenching temperature and holding time have a significant effect on the tensile fracture morphology of B1500HS quenchable high-strength boron steel.

Several researchers have studied the fracture morphologies of steels at low or high temperatures. DU et al [14] described the fracture behaviour of a 9 % nickel 1000 MPa-grade high-strength steel using tensile tests at low temperatures. Four critical stresses were found, which determines the fracture behaviour at various temperatures. SHI et al [15] investigated the fracture morphologies of 22SiMn2TiB and indicated that

Foundation item: Project(51305317) supported by the National Natural Science Foundation of China; Projects(WUT: 2013-IV-092, WUT: 2014-VII-002) supported by the Fundamental Research Funds for the Central Universities, China; Project(IRT13087) supported by Innovative Research Team Development Program of Ministry of Education of China
Received date: 2014−03−02; **Accepted date:** 2014−09−12
Corresponding author: SONG Yan-li, Associate Professor, PhD; Tel: +86−15527510094; E-mail: yanlisong@whut.edu.cn, ylsong2012@126.com

the fracture can be described as being more ductile at 700 ºC than at 600 ºC. LOPEZ-CHIPRES et al [16] and MEJIA et al [17] reported the influence of boron contents on the hot ductility and the fracture morphology of boron microalloyed steels. The experimental results showed that the hot ductility of the steels microalloyed with boron compares favourably to that without boron addition. HE et al [18] derived a new ductile fracture criterion for 30Cr2Ni4MoV steel by taking into account the plastic deformation capacity of the material and stress states.

Based on the above analysis, we can see that the study of the fracture behaviour of the steel sheets has mainly focused on room-temperature conditions, with high temperatures receiving less attention. Moreover, few studies have addressed the fracture mechanisms of high-strength boron steels at elevated temperatures or have linked the fracture behaviour of steel sheets to the microstructure transformation. In this work, the fracture morphologies and fracture mechanisms of high-strength boron steel at different temperatures were investigated.

2 Experimental procedure

2.1 Material and specimens

High-strength boron steel specimens (1.8 mm thick) were employed with the chemical composition of the specimens listed in Table 1. The microstructure is comprised of ferrite and pearlite.

Table 1 Chemical composition of high-strength boron steel (mass fraction, %)

C	Si	Mn	P	S	Cr	Ti	B	N	Others.
0.23	0.22	0.18	0.015	0.001	0.16	0.04	0.003	0.005	Bal.

2.2 Uniaxial tensile tests

The uniaxial tensile specimens were prepared by wire-electrode cutting, and the length direction is along their rolling directions. The isothermal tensile tests were performed at different temperatures on the Gleeble 3500 thermal-simulating machine shown in Fig. 1. The test scheme is shown in Table 2 and Fig. 2. Specifically, the specimens were heated to 900 ºC at a rate of 10 ºC/s and maintained for 5 min to obtain full austenite. The specimens were then cooled to the deformation temperatures (600−900 ºC) at a cooling rate of 30 ºC/s and isothermally pulled at a strain rate of 0.1 s^{-1}. As a contrast test, the specimen at 25 ºC was pulled directly without being heated at a strain rate of 0.1 s^{-1}. After fracture, the broken specimens were quenched by water and the cooling rate was higher than 500 ºC/s. To accurately measure the temperature, heating time and cooling rate, two K-type thermocouples were welded on the surface of the central region of every specimen by spot-welding before the tests. The distance between the two thermocouples was 1−2 mm.

Fig. 1 Gleeble 3500 thermal-simulating machine

Table 2 Isothermal tensile test scheme of high-strength boron steel specimens at 600−900 °C

No.	T_1/°C	T_2/°C	Strain rate/s^{-1}
1−3	900	900	0.1
4−6		800	
7−9		750	
10−12		700	
13−15		650	
16−18		600	

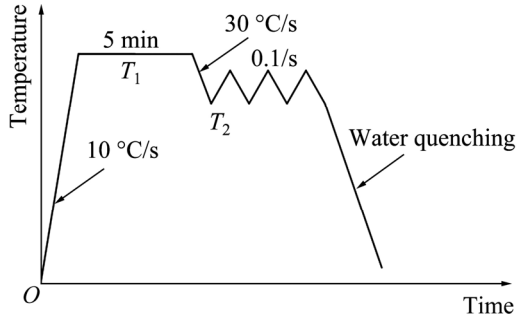

Fig. 2 Temperature history of high-strength boron steel specimens at 600−900 °C

2.3 Morphological observation of fractures

As shown in Fig. 3, specimens with the length of 15 mm were cut from the homogenous deformation zone. The specimens were wrapped with cloth or paper to prevent from pollution during the cutting process. The fracture morphologies were observed using a Quanta 200 scanning electron microscope.

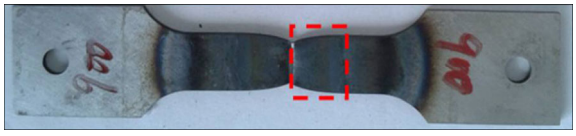

Fig. 3 Dissected position of a specimen

2.4 Metallographic observation of fractures

Specimens (5 mm×15 mm) were cut along the longitudinal profile line of the specimens for metallographic observation. The specimens were ground with abrasive paper and polished using a woollen cloth with diamond paste, and the microstructures were determined using a ULTRA plus field emission scanning electron microscope (SEM).

3 Results and discussion

3.1 Tensile test results

The fractured specimens are shown in Fig. 4 and the true stress–true strain curves at different temperatures at a strain rate of 0.1 s^{-1} for the high-strength boron steel specimens are shown in Fig. 5. The influence of the deformation temperature on the flow stress is clearly serious; the flow stress expresses a dynamic flow softening behaviour at 650 ℃−900 ℃ and work hardening behaviour at 25 ℃ and 600 ℃. During the tensile tests, the flow stress decreases with increasing deformation temperature at a given strain [19]. It also indicates an increasing deformation temperature, leading to a apparent decrease of the slope of the true stress−true strain curves within the plastic deformation range. At deformation temperatures higher than 650 ℃, the material exhibits dynamic recrystallization and recovery processes. This leads to a tendency of the sheet metal to exhibit a plane flow curve characteristic after the initial strain hardening, which is more apparent as the temperature increases. The similar tendency can also be found in the work by MERKLEIN and LECHLER [20].

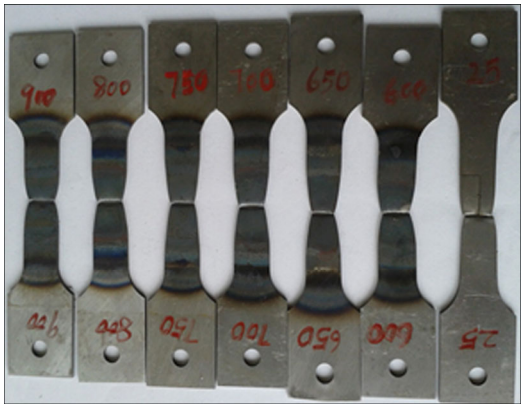

Fig. 4 Specimens after tensile tests

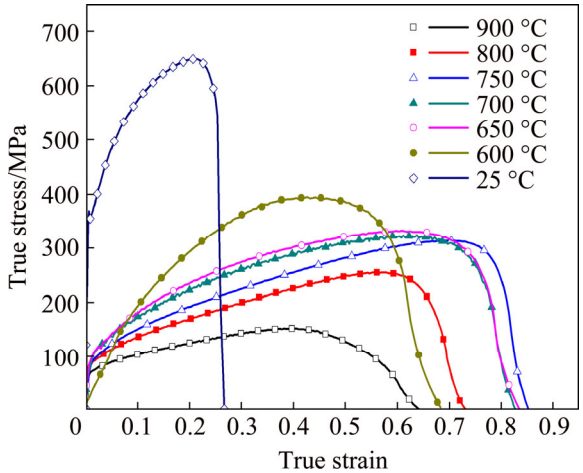

Fig. 5 True stress−true strain curves at different temperatures at strain rate of 0.1 s^{-1}

3.2 Fracture morphologies

3.2.1 Comparison of fracture morphologies on centre of ductile fracture

To describe the flow behaviour of the high-strength boron steel, the fracture morphologies of the specimens were observed. The analysis of the feature of the fracture denotes that plastic deformation has occurred in all of the specimens [15]. Figure 6 compares the fracture morphologies at the centre of the ductile fracture of the high-strength boron steel specimens deformed at different temperatures. Necking can be observed in the tensile fracture of high-strength boron steel, and the neck section is perpendicular to the direction of the principal strain. Furthermore, the reduction of the material thickness of the fracture zone is relatively large, and the whole fracture is the shear plane. The centre of the ductile fracture exhibits secondary cracks and parabolic shear dimples, which divides the whole section into two parts. This demonstrates that the specimens have good plasticity at high temperatures [15].

As can be observed in the enlarged morphologies of Fig. 6, for the tensile specimens at elevated temperatures, the dimple number decreases as the deformation temperature increases at a constant strain rate, meaning that the fracture hole number decreases, the glide step number around the dimple increases and the aggregation and growth of the microvoids enhance. The length ratio of dimple to fracture is estimated using the following equation:

$$k_{\mathrm{d}}=\frac{l_{\mathrm{d}}}{l}\times 100\% \tag{1}$$

where k_{d} corresponds to the length ratio of dimple to fracture; l_{d} and l are the lengths of the dimple and fracture, respectively.

The effect of temperature on k_{d} is illustrated in Fig. 7. Obvious snake glide lines on the dimples are shown in Figs. 6(e) and (f), illustrating that the glide phenomenon is more evident at 600−650 ℃ than at other temperatures. Based on the above analysis, it also can be obtained that there are some differences between the fracture morphologies at higher temperatures and lower

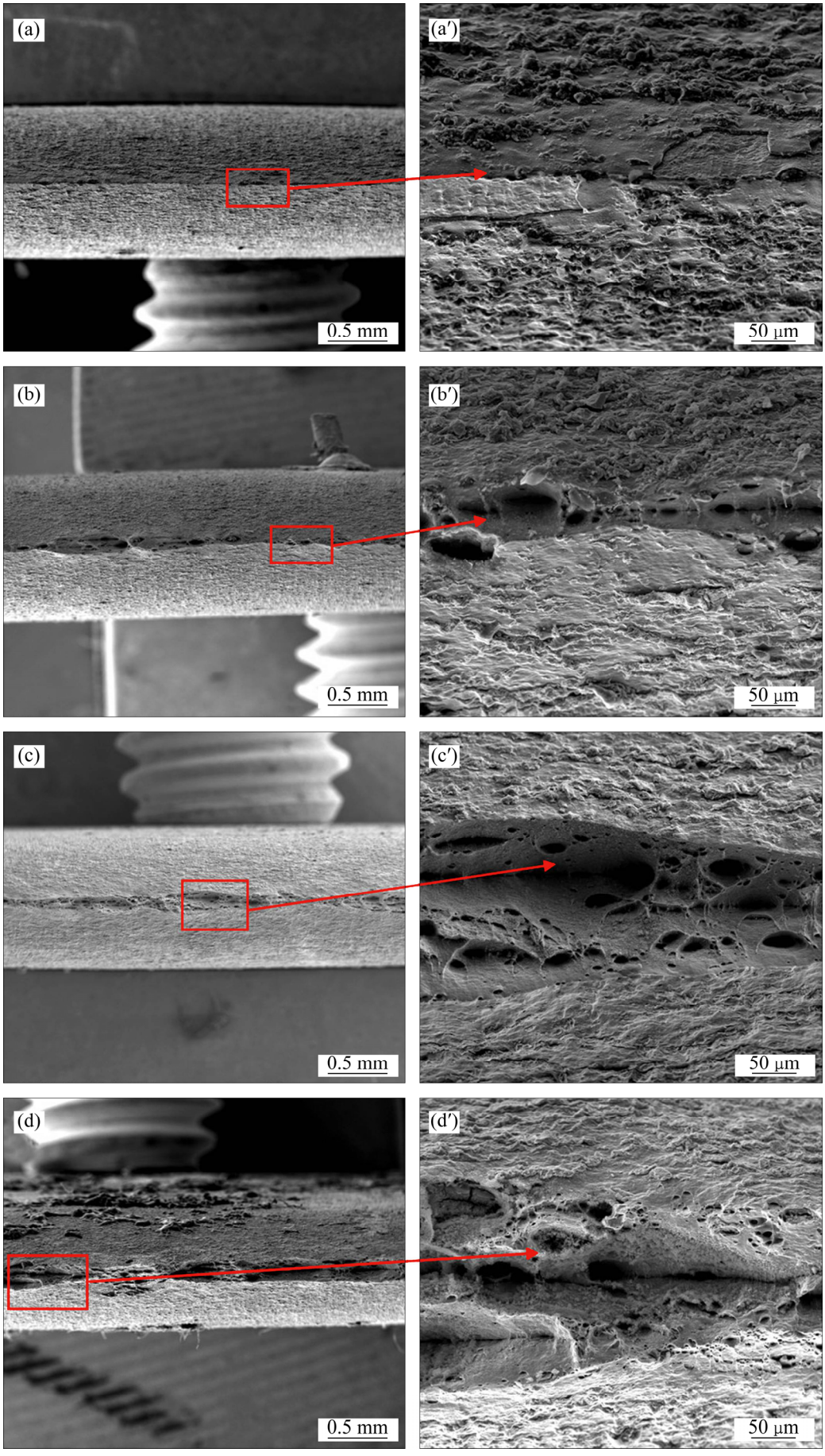

to be continued

continue

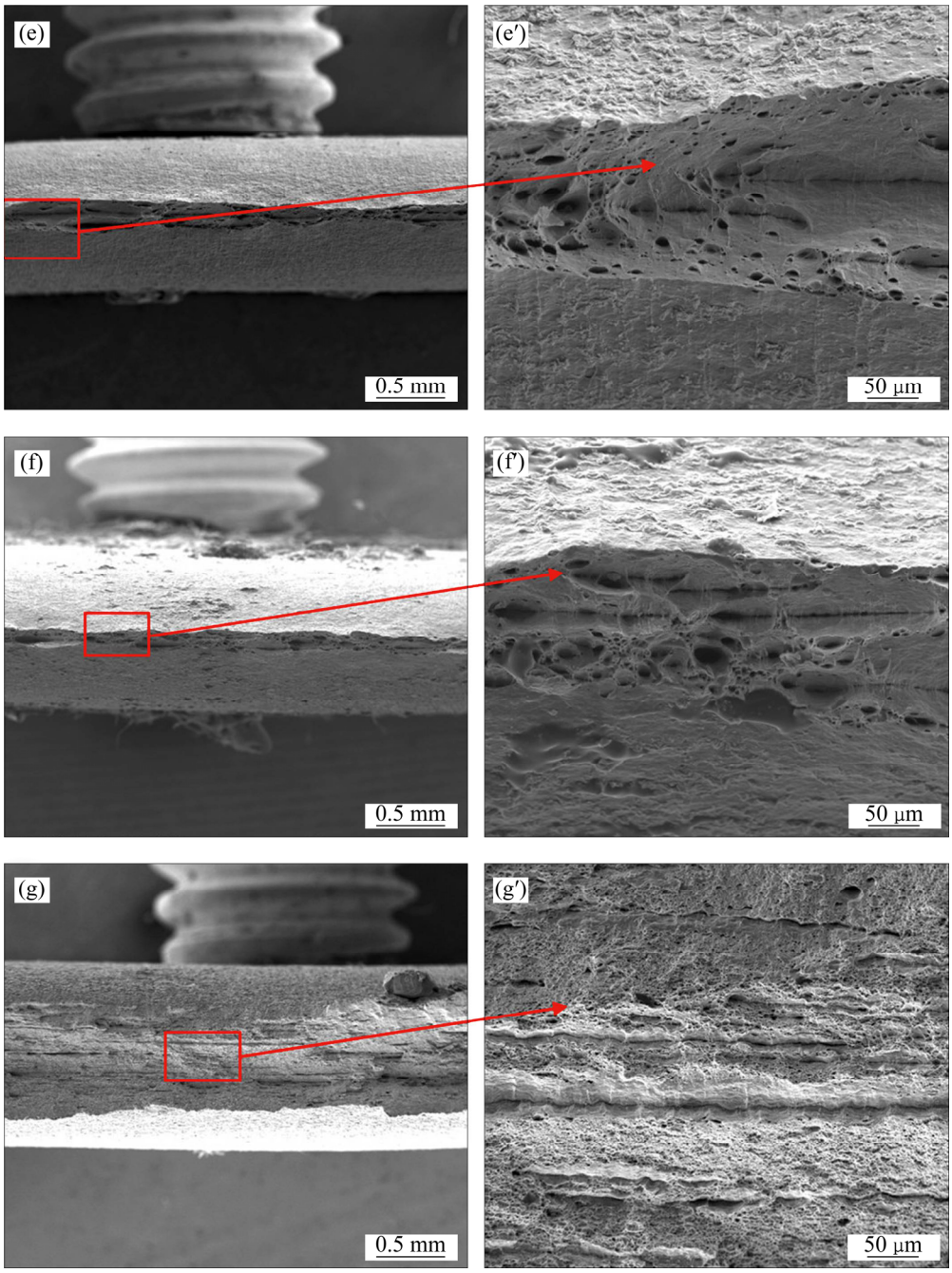

Fig. 6 Fracture morphologies on centre of ductile fracture of high-strength boron steel as-quenched specimens deformed at different temperatures: (a, a') 900 °C; (b, b') 800 °C; (c, c') 750 °C; (d, d') 700 °C; (e, e') 650 °C; (f, f') 600 °C; (g, g') 25 °C

temperatures. This difference may be attributed to different deformation temperatures leading to different microstructures; therefore, it is necessary to study the microstructure of the fracture zone. Comparing Fig. 6(g) with Figs. 6(a)−(f), there are obvious differences between the fracture morphologies at room temperature and high temperatures. The fracture of the central zone at room temperature exhibits large circular dimples and tearing traces, corresponding to lamellar fractures. The crack beginning in the rolling defects is a pearlite fracture. However, the fracture of the upper and lower sides, having finer dimples, is a ferrite fracture, as shown in Fig. 6(g). It has been commonly reported that lamellar fractures are related to the banded structure of steel sheets, which includes bands of ferrite and pearlite. Owing to differences in the mechanical properties of ferrite and pearlite, the deformation in tensile tests cannot be of coordination. Thus, the fracture occurs earlier in the less plastic pearlite because of transformation hysteresis, i.e., micro-cracking. The

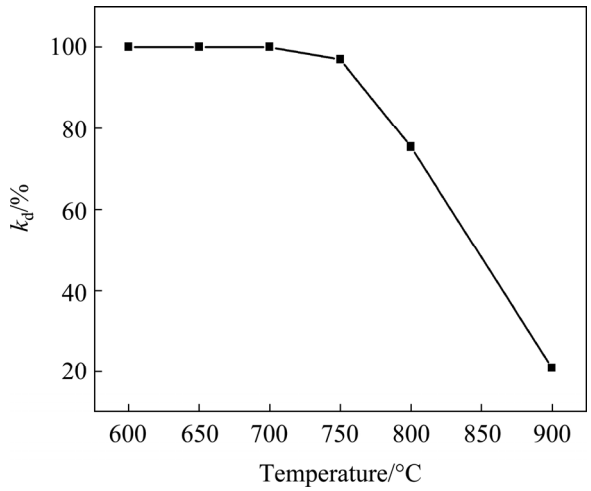

Fig. 7 Length ratio of dimple to fracture of high-strength boron steel as-quenched specimens deformed at different temperatures

micro-crack extends along the interface of pearlite and ferrite and then gradually develops into a lamellar shape [21].

To further study the isothermal tensile fracture behaviour of high-strength boron steel, the fracture dimples and oxide morphologies of the different zones of specimen at 600 ºC are compared in Fig. 8. It can be inferred that the centre of the specimen is fractured in advance, as the oxide around the secondary cracks and dimples at the end of the ductile fracture is thinner than that at the center. Moreover, the tearing ridges and glide lines at the end of the ductile fracture are more evident than that at the centre. Because the tensile force is larger, the fracturing is slower and the exposed time is longer when the specimen is fractured first, more oxide skin is formed. This finding indicates that the fracture begins at the centre of the specimen and then extends to the end during the isothermal tensile test.

3.2.2 Comparison of fracture morphologies at end of ductile fracture

As shown in Fig. 9, for the tensile specimens at elevated temperatures (except at 700 ºC), the length of the remelting zone at the end of the specimens increases as the deformation temperature increases under a constant strain rate. Higher temperatures need higher currents and therefore more severe remelting at the end of the specimens (see Fig. 10). The length of the remelting zone at the end of the specimens is the longest at 700 ºC, which might be due to the broken specimens colliding with each other because of inertia at the end of the tensile test. Furthermore, the higher the temperature is, the less the dimples are present. When the temperature is 900 ºC, the end of the ductile fracture exhibits an

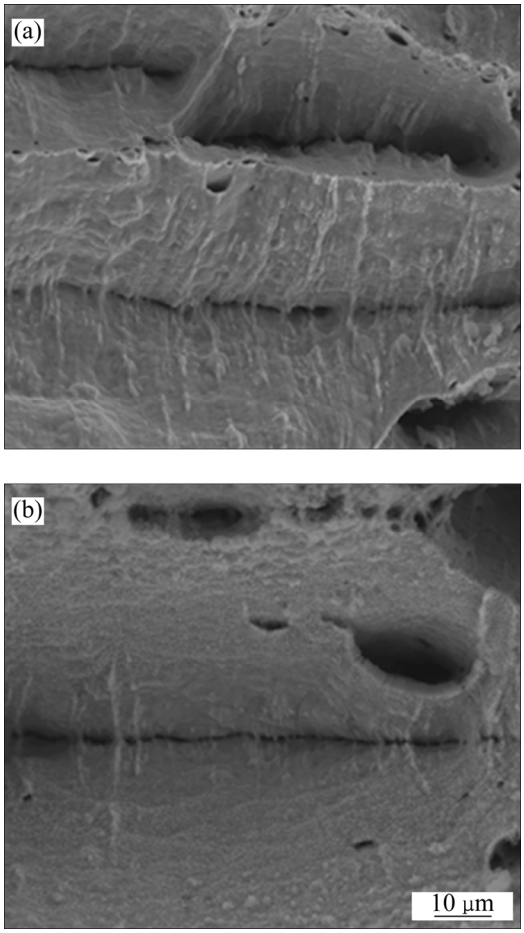

Fig. 8 Comparison of fracture dimples and oxide morphologies of high-strength boron steel as-quenched specimen at 600 °C: (a) End; (b) Centre

obvious plastic elongation band, meaning that larger plastic deformation appears at the end. The length of the remelting zone of the end of the specimens at room temperature is the smallest, as the current through the specimen is the lowest at room temperature.

3.2.3 Comparison of oxide morphologies on ductile fracture

The oxide on the surface affects the performance of the steel sheets formed in a high-temperature atmosphere. Thus, the study of the effect of temperature on the oxide skin is necessary. The oxide morphologies on the ductile fracture of the high-strength boron steel specimens formed at different temperatures are shown in Fig. 11.

It can be found that the higher the temperature is, the thicker and more compact the oxide is, and vice versa. In addition, the end of the oxide becomes more spinous and more laminated at lower temperatures. Thus, high temperatures increase the oxidation degree of the steel sheets, even causing the oxide to shed, which makes the steel thinner and weaker. Thus, overly high temperatures are not beneficial for the formation of steel sheets.

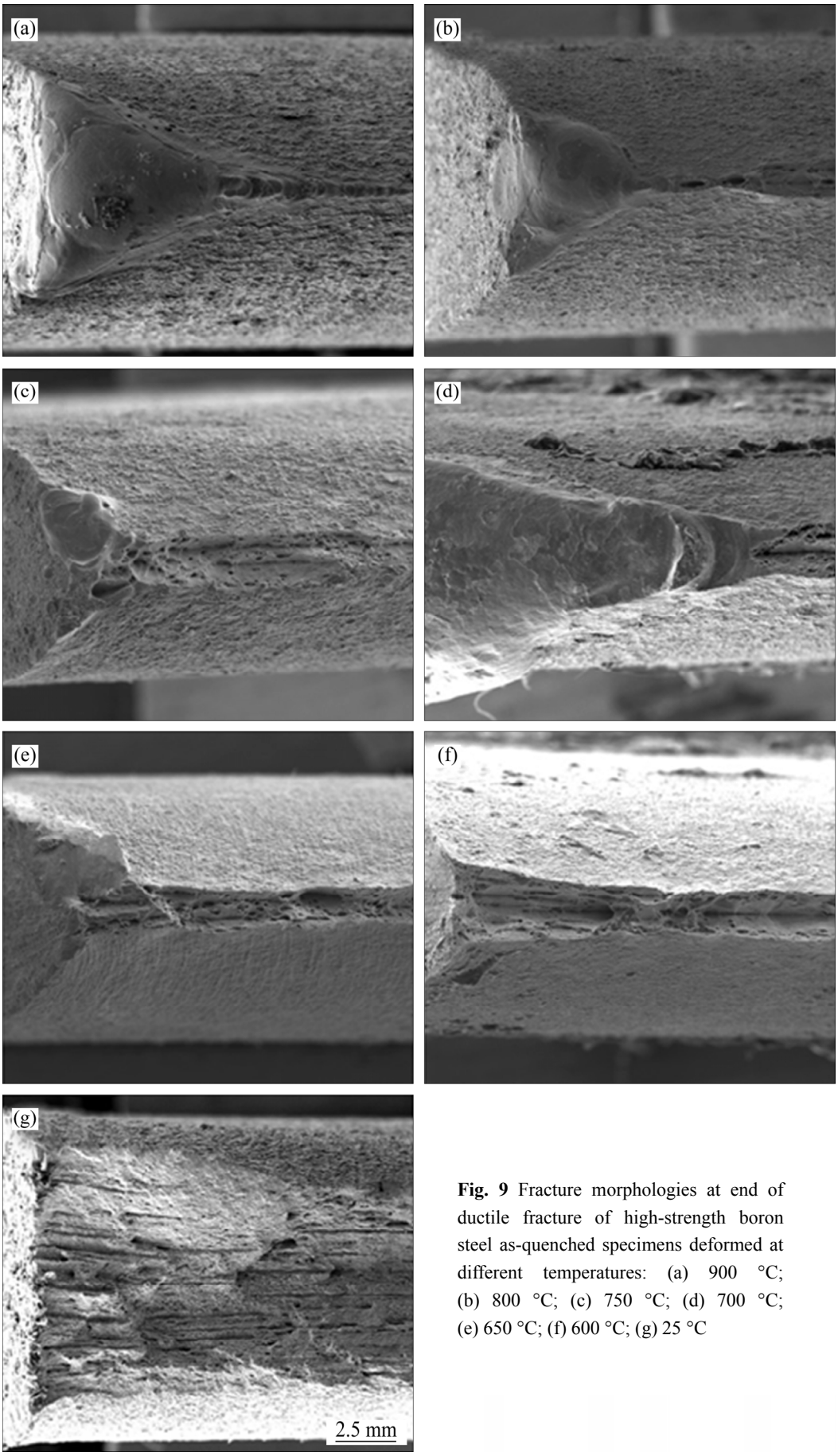

Fig. 9 Fracture morphologies at end of ductile fracture of high-strength boron steel as-quenched specimens deformed at different temperatures: (a) 900 °C; (b) 800 °C; (c) 750 °C; (d) 700 °C; (e) 650 °C; (f) 600 °C; (g) 25 °C

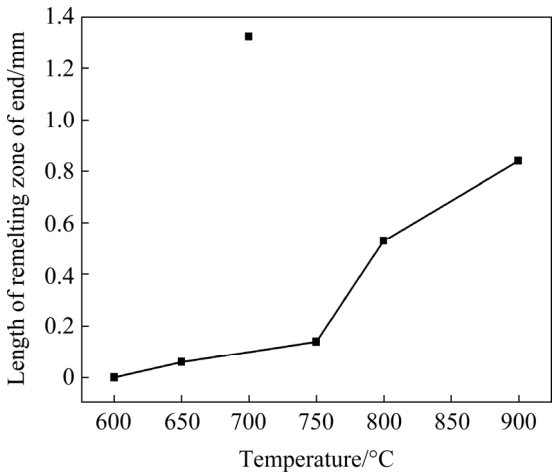

Fig. 10 Length of remelting zone at end of high-strength boron steel as-quenched specimens deformed at different temperatures

3.3 Fracture microstructure

By analyzing the fracture morphologies at the centre and end of the ductile fracture and the oxide morphologies of the high-strength boron steel specimens deformed at different temperatures, it can be found that the deformation temperature has a strong effect on the fracture morphology. In addition, the fracture morphologies are closely related to the microstructure; thus, analyzing the microstructure of the tensile fracture zone is essential. At 600 ºC−900 ºC, combined with the CCT curves of the high-strength boron steel shown in Fig. 12 [22] and the isothermal tensile conditions, the morphologies qualitatively indicate that the lower the temperature is, the more the ferrite and bainite are formed, which in turn increases the plasticity and the number of dimples.

SEM micrographs of high-strength boron steel specimens deformed at different temperatures are shown in Fig. 13. It can be deduced that the SEM morphology is characterized by lath martensite at 900 ºC−800 ºC (see Figs. 13(a) and (b)). However, at 750 ºC, in addition to lath martensite formed inside the austenite grain, polygonal ferrite formed at the prior austenite grain boundaries is also found in the specimen (see Fig. 13(b)). The isothermal deformation in the austenite promotes the formation of the granular bainite and a little acicular ferrite forms in the interior of the austenite grain when the deformation temperature is 700 ºC [15]. Furthermore, the microstructure is comprised of lath martensite, acicular ferrite and granular bainite at deformation temperatures of 600 ºC−650 ºC (see Figs. 13(c)−(f)). The microstructure of the specimen is pearlite and ferrite at room temperature; thus, the fracture morphology is characteristic of typical lamellar tearing and exhibits a delamination shape.

SHI et al [15] pointed out that the isothermal deformation in the metastable austenite phase accelerated the diffusion transformations at 600 ºC−800 ºC and especially stimulated the long-range diffusion of carbon atoms in austenite. In this work, however, the diffusion transformations were observed within the deformation temperature range of 600−750 ºC. Additionally, under a cooling rate of 30 ºC/s, full martensite cannot be acquired. Therefore, to obtain full martensite, a higher cooling rate is needed. The influence of deformation temperature on the diffusion transformations can be explained from the following aspects. First, decreasing temperature leads to increasing driving force of the diffusion transformations. Secondly, at a certain strain level and strain rate, decreasing deformation temperature results in the increase of flow stress and then more stored energy is introduced into the austenite, which activates the ferrite growing from austenite grain boundaries into the austenite grain and then parallel platelets [15, 23]. Resultantly, the appearance of ferrite changes from polygonal ferrite to acicular ferrite. In addition, the diffusion transformations continue to nucleate and grow in the condition that the cooling time is sufficient. For a constant cooling rate, a lower deformation temperature brings out more diffusion transformations as more time is available for deformation. Hence, the ferrite and granular bainite volume fractions of the specimens increase and the martensite volume fraction decreases as the deformation temperature decreases (see Fig. 14).

According to MIN et al [23] and KIRKALDY et al [24], the B_s and M_s can be estimated as 614 ºC and 443 ºC by Eqs. (2) and (3), respectively. The transformation temperature of austenite to granular bainite, however, is found to increase to about 700 ºC in this experiment. The start temperatures of bainite and martensite are given as

$$T_{bs}=656-58w(C)-35w(Mn)-75w(Si)-15w(Ni)-34w(Cr)-41w(Mo) \quad (2)$$

$$T_{ms}=561-474w(C)-35w(Mn)-17w(Ni)-17w(Cr)-21w(Mo) \quad (3)$$

The elongation of high-strength boron steel specimens at elevated temperatures can be calculated as Eq. (4). As we can see from Fig. 15, as the deformation temperature increases, the elongation of high-strength boron steel specimens first increases and then decreases. When the deformation temperature is 750 ºC, the greatest elongation is obtained, meaning that the investigated steel has the best plasticity when the deformation temperature is 750 ºC. The reason is that the plasticity of polygonal ferrite is better than that of austenite OR granular bainite, thus a little polygonal ferrite can increase the elongation when the temperature is lower than 750 ºC; the elongation decreases as the combination

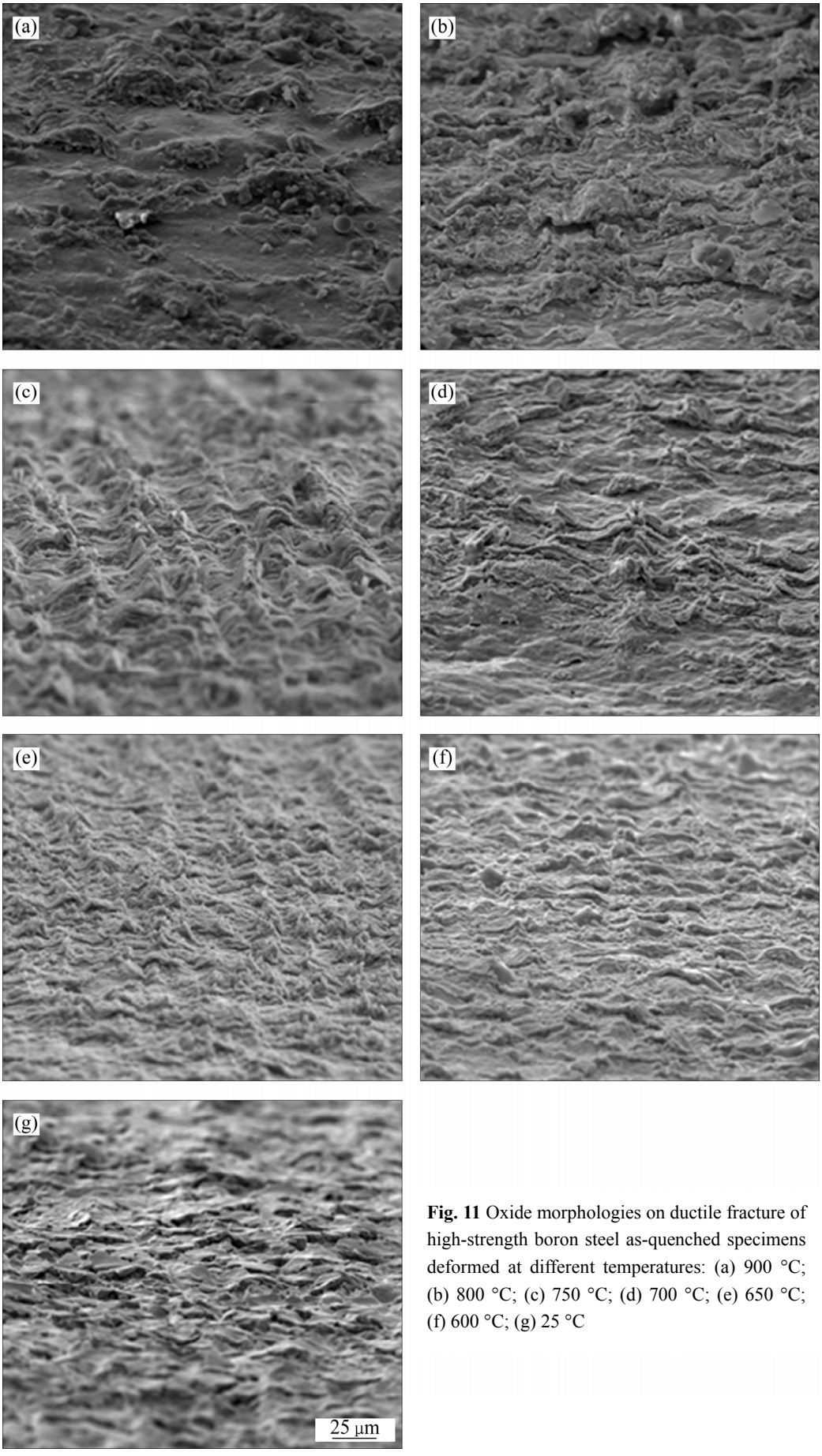

Fig. 11 Oxide morphologies on ductile fracture of high-strength boron steel as-quenched specimens deformed at different temperatures: (a) 900 °C; (b) 800 °C; (c) 750 °C; (d) 700 °C; (e) 650 °C; (f) 600 °C; (g) 25 °C

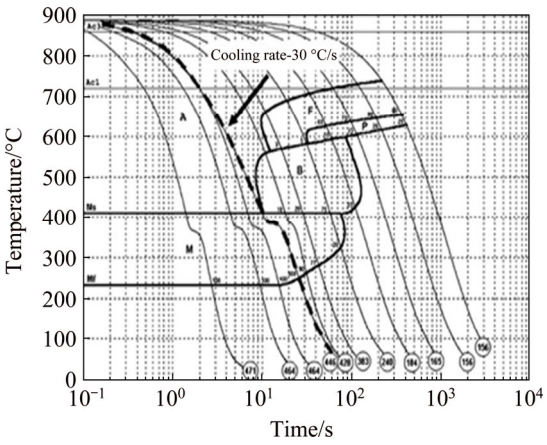

Fig. 12 CCT curves of high-strength boron steel [22]

of ferrite and granular bainite is harmful to the toughness. Once the deformation temperature rises to 800 ºC, the elongation decreases again due to the disappearance of polygonal ferrite.

$$\delta = \frac{l_1 - l_0}{l_0} \tag{4}$$

where δ is the elongation of the high-strength boron steel; l_1 and l_0 are the final and original gauge lengths, respectively. The value of l_0 (the length of the homogenous temperature zone) is 7−8 mm when the deformation temperatures are 600 ºC−900 ºC; while it is 38.1 mm when the deformation temperature is 25 ºC.

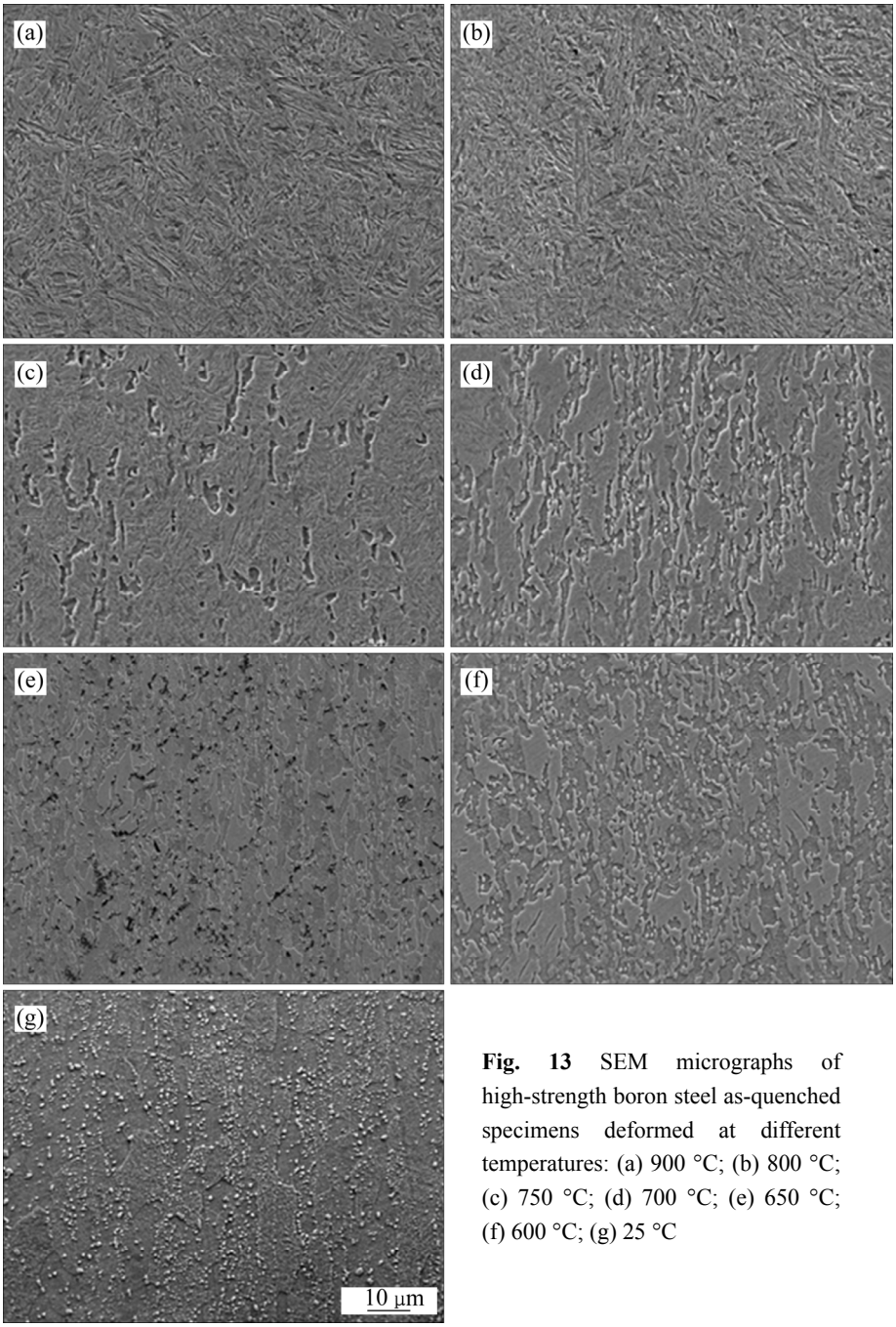

Fig. 13 SEM micrographs of high-strength boron steel as-quenched specimens deformed at different temperatures: (a) 900 °C; (b) 800 °C; (c) 750 °C; (d) 700 °C; (e) 650 °C; (f) 600 °C; (g) 25 °C

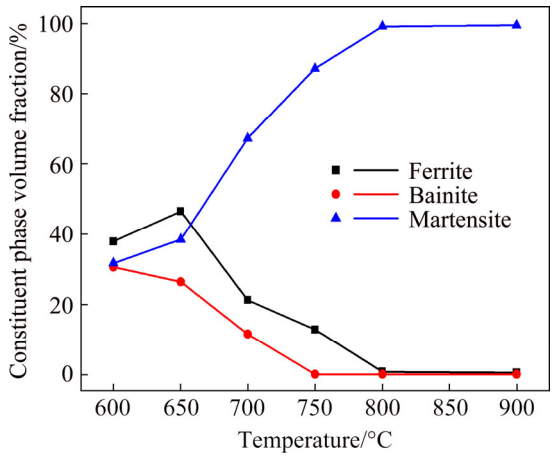

Fig. 14 Constituent phases volume fractions of high-strength boron steel as-quenched specimens deformed at different temperatures: (a) 900 °C; (b) 800 °C; (c) 750 °C; (d) 700 °C; (e) 650 °C; (f) 600 °C

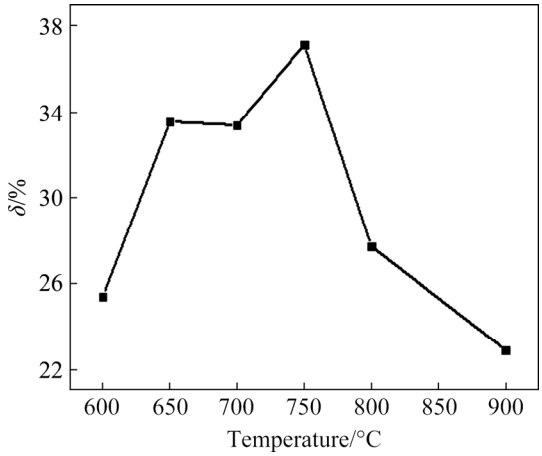

Fig. 15 Elongation of high-strength boron steel as-quenched specimens deformed at different temperatures

4 Conclusions

1) High temperatures produce a dimple fracture, which proves that high-strength boron steel exhibits good plasticity at high temperatures. The fracture of the high-strength boron steel specimens begins at the centre and then extends to the end of the specimen during the isothermal tensile test. Ferrite is observed in dimple fractures whereas pearlite cracks in a fingerprint pattern.

2) At 600−900 ℃, the length ratio of dimple to fracture decreases, the length of the remelting zone at the end increases and the oxide becomes thicker and more compact as the deformation temperature increases.

3) The fracture morphologies of the high-strength boron steel specimens are closely related to the microstructure. Isothermal deformation in the metastable austenite phase accelerates the diffusion transformations within the range of 600−750 ℃. Thus, to obtain full martensite, a higher cooling rate is needed.

4) A greatest elongation of the high-strength boron steel is achieved when the deformation temperature is 750 ℃ due to the existence of polygonal ferrite.

References

[1] DANCETTE S, FABREGUE D, ESTEVEZ R, MASSARDIER V, DUPUY T, BOUZEKRI M. A finite element model for the prediction of advanced high strength steel spot welds fracture [J]. Eng Fract Mech, 2012, 87: 48−61.

[2] KARBASIAN H, TEKKAYA A E. A review on hot stamping [J]. J Mater Process Tech, 2010, 210: 2103−2118.

[3] MORI K, OKUDA Y. Tailor die quenching in hot stamping for producing ultra-high strength steel formed parts having strength distribution [J]. CIRP Ann-Manuf Tech, 2010, 59: 291−294.

[4] HUA Lin, MENG Fan-zhi, SONG Yan-li, LIU Jia-ning, QIN Xun-peng, SUO Lian-bing. A constitutive model of 6111-T4 aluminum alloy sheet based on the warm tensile test [J]. J Mater Eng Perform, 2014, 23(3): 1107−1113.

[5] TOROS S, POLAT A, OZTURK F. Formability and springback characterization of TRIP800 advanced high strength steel [J]. Mater Des, 2012, 41: 298−305.

[6] SONG Yan-li, HUA Lin, CHU Dong-ning, LAN Jian. Characterization of the inhomogeneous constitutive properties of laser welding beams by the micro-Vickers hardness test and the rule of mixture [J]. Mater Des, 2012, 37(5): 19−27.

[7] SONG Yan-li, HUA Lin. Influence of inhomogeneous constitutive properties of weld materials on formability of tailor welded blanks [J]. Mater Sci Eng A, 2012, 552(8): 222−229.

[8] SONG Yan-li, HUA Lin, MENG Fan-zhi. Inhomogeneous constructive modeling of laser welded bead based on nanoindentation test [J]. Ironmak Steelmak, 2012, 39(2): 95−103.

[9] GHOSH S, DAS G. Effect of pre-strain on the indentation fracture toughness of high strength low alloy steel by means of continuum damage mechanics [J]. Eng Fract Mech, 2012, 79: 126−137.

[10] WANG Wu-rong, LI Meng, HE Chang-wei, WEI Xi-cheng, WANG Da-zhi, DU Han-bin. Experimental study on high strain rate behavior of high strength 600−1000 MPa dual phase steels and 1200 MPa fully martensitic steels [J]. Mater Des, 2013, 47: 510−521.

[11] ARPAN D, SOUMITRA T. Experimental investigation on martensitic transformation and fracture morphologies of austenitic stainless steel [J]. Int J Plasticity, 2009, 25: 2222−2247.

[12] LU J Z, ZHONG J S, LUO K Y, ZHANG L, QI H, LUO M, XU X J, ZHOU J Z. Strain rate correspondence of fracture surface features and tensile properties in AISI304 stainless steel under different LSP impact time [J]. Surf Coat Tech, 2013, 221: 88−93.

[13] HE Lian-fang. Research on key parameter measuring and quenching properties of boron steel B1500HS in hot stamping process [D]. Jinan: Shandong University, 2012. (in Chinese)

[14] DU W S, CAO R, YAN Y J, TIAN Z L, PENG Y, CHEN J H. Fracture behavior of 9% nickel high-strength steel at various temperatures Part I. Tensile tests [J]. Mater Sci Eng A, 2008, 486: 611−625.

[15] SHI Zeng-min, LIU Kai, WANG Mao-qiu, SHI Jie, DONG Han, PU Jian, CHI Bo, ZHANG Yi-sheng, LI Jian. Thermo-mechanical properties of ultra high strength steel 22SiMn2TiB at elevated temperature [J]. Mater Sci Eng A, 2011, 528: 3681−3688.

[16] LOPEZ-CHIPRES E, MEJIA I, MALDONADO C. Hot ductility behavior of boron microalloyed steels [J]. Mater Sci Eng A, 2007, 460−461: 464−470.

[17] MEJIA I, BEDOLLA-JACUINDE A, MALDONADO C. Hot ductility behavior of a low carbon advanced high strength steel (AHSS) microalloyed with boron [J]. Mater Sci Eng A, 2011, 528:

4468−4474.

[18] HE Jian-li, CUI Zhen-shan, CHEN Fei, XIAO Yan-hong, RUAN Li-qun. The new ductile fracture criterion for 30Cr2Ni4MoV ultra-super-critical rotor steel at elevated temperatures [J]. Mater Des, 2013, 52: 547−555.

[19] YU Bao-jun, GUAN Xiao-jun, WANG Li-jun, ZHAO Jian, LIU Qian-qian, CAO Yu. Hot deformation behavior and constitutive relationship of Q420qE steel [J]. Journal of Central South University, 2011, 18(1): 36−41.

[20] MERKLEIN M, LECHLER J. Investigation of the thermo-mechanical properties of hot stamping steels [J]. J Mater Process Tech, 2006, 177(1/2/3): 452−455.

[21] DEREK H. Fractography observing, measuring and interpreting fracture surface topography [M]. Cambridge: Cambridge University Press, 1999: 233−239.

[22] NADERI M, DURRENBERGER L, MOLINARI A, BLECK W. Constitutive relationships for 22MnB5 boron steel deformed isothermally at high temperatures [J]. Mater Sci Eng A, 2008, 478(1/2): 130−139.

[23] MIN Jun-ying, LIN Jian-ping, MIN Yong-an, LI Fang-fang. On the ferrite and bainite transformation in isothermally deformed 22MnB5 steels [J]. Mater Sci Eng A, 2012, 550: 375−387.

[24] KIRKALDY J S, VENUGOPALAN D. Prediction of microstructure and hardenability in low alloy steels [C] // MARDER A R, GOLDSTEIN J I. Proceedings of an International Conference on Phase Transformations in Ferrous Alloys. Philadelphia: Metallurgical Society of AIME, 1984: 125−148.

(Edited by FANG Jing-hua)